First-in-human Study of a ^{99m}Tc-Labeled Single-Domain Antibody for SPECT/CT Assessment of HER2 Expression in Breast Cancer

Lingzhou Zhao
Shanghai Jiao Tong University School of Medicine
Changcun Liu
Shanghai Jiao Tong University School of Medicine
Yan Xing
Shanghai Jiao Tong University School of Medicine
Jin He
Shanghai Jiao Tong University School of Medicine
Jim O'Doherty
Siemens Healthineers
Wenhua Huang
Nanomab Technology Limited
Jinhua Zhao (zhaojinhua1963@126.com)
Shanghai General Hospital, Shanghai Jiao Tong University School of Medicine https://orcid.org/0000-0002-8867-7985

Research

Keywords: HER2 imaging, breast cancer, single-domain antibody, SPECT/CT

Posted Date: March 31st, 2021

DOI: https://doi.org/10.21203/rs.3.rs-356098/v1

Abstract

Background: Accurate determination of human epidermal growth factor receptor 2 (HER2) expression is essential for HER2-targeted therapy. HER2 expression in a complex environment, such as in a heterogenous tumor, makes precise assessment difficult using current methods. Therefore, we developed a novel ^{99m}Tc-labeled anti-HER2-single domain antibody (^{99m}Tc-NM-02) as a molecular imaging tracer for non-invasive detection of HER2 expression and investigated its safety, radiation dosimetry, biodistribution, and tumor-targeting potential in breast cancer patients.

Methods: A lead compound (NM-02) was screened from a library of hexahistidine-tagged anti-HER2-single domain antibodies and labeled with ^{99m}Tc for the preparation of ^{99m}Tc-NM-02 tracer. Ten women with breast cancer were administered ^{99m}Tc-NM-02 at a mean dose of 458 ± 37 MBq (406–510 MBq), corresponding to 100 μg of NM-02. Whole-body and local SPECT/CT images were acquired at 1 and 2 h post-administration to investigate the tumor-targeting potential in primary and metastatic lesions. Additional images were acquired at 10 min, 3 h, and 24 h in three patients to calculate radiation dosimetry. Physical evaluation and blood analysis were performed for safety assessment.

Results: No drug-related adverse reactions occurred. The tracer mainly accumulated in the kidneys and liver with mild uptake in the spleen, intestines, and thyroid, but only background levels were observed in other organs where primary tumors and metastases typically occurred. The mean effective dose was 6.56×10^{-3} mSv/MBq, and tracer uptake was visually observed in primary tumors and metastases. Owing to the fast clearance of the tracer, we were able to sufficiently discern uptake over normal background in both primary lesions and metastases within 2 h after injection. A maximal standard uptake value of 1.5 could be a reasonable cutoff for determining HER2 positivity using SPECT/CT imaging.

Conclusions: Our ^{99m}Tc-NM-02 tracer can be safely used for imaging in breast cancer patients with reasonable radiation doses, favorable biodistribution and imaging characteristics. ^{99m}Tc-NM-02 SPECT imaging may provide an accurate and non-invasive method to detect HER2 status in breast cancer patients.

Trial registration: ClinicalTrials.gov, NCT04040686. Registered 30 July 2019. https://clinicaltrials.gov/ct2/show/NCT04040686.

Background

Breast cancer has become the most common cancer in women worldwide [1–3]. One in eight women will be diagnosed with breast cancer in her life. Breast cancers can be classified into cancer subtypes based on the expression of molecular biomarkers, which allows physicians to adjust treatment plans and response assessments for improved survival and morbidity [4–6]. This development in breast cancer diagnosis and treatment has led to an evolution from standard strategies to precision medicine [7]. In addition to hormone receptors, human epidermal growth factor receptor 2 (HER2), which is highly expressed in about 20% of breast cancer patients, is a crucial biomarker for breast cancer classification [8, 9]. These patients usually respond poorly to endocrine therapy and chemotherapy but obtain a marked survival benefit from HER2-targeted therapy [9–11]. Therefore, accurate determination of HER2 expression is a primary concern when selecting therapy.

Immunohistochemistry (IHC) and fluorescence in situ hybridization (FISH) of tumor tissues are routinely performed in the clinic to determine HER2 expression. Based on pathology results, breast cancer patients who have strong overexpression of HER2 (HER2 3+) or amplification of *HER2/neu* (FISH +) are suitable for HER2-targeted therapy, because they will gain the most clinical benefits from this treatment [12]. The guidelines for HER2 testing have been revised several times to improve the accuracy and reproducibility of the interpretation of HER2 status [13]. However, despite these revisions, multiple studies have shown inaccurate HER2 testing results for breast cancer patients. The discordance rate was reported to be as high as 20% in an early study [14], although it had decreased to less than 10% in a more recent study [15]. Nevertheless, incorrect classification of HER2 status may lead clinicians to not administer anti-HER2 therapy when it might be effective and, conversely, increase needless cost and prolonged treatment for patients with false-positive results. With the increasing administration of HER2-directed therapies, the accurate determination of HER2 expression is critical.

Single-domain antibodies (sdAbs) are small antigen-binding fragments that are naturally derived from heavy-chain-only antibodies and are mainly produced in camelids [16]. Due to the outstanding features, such as fast blood clearance, deep tissue penetration, and high affinity, sdAbs are identified as ideal candidates for nuclear medicine applications [16, 17]. Several studies have demonstrated the safety and feasibility of radiolabeled sdAbs for cancer diagnosis and treatment [18–26]. In our previous study, we reported a ^{99m}Tc-labeled anti-programmed death ligand-1 (PD-L1) sdAb as a SPECT/CT tracer for PD-L1 expression in non-small cell lung cancer (NSCLC) [26]. The tracer had an excellent safety profile, favorable imaging characteristics, and a significant correlation with PD-L1 IHC results in NSCLC

patients. Here, we used another novel sdAb (NM-02) to develop a ^{99m}Tc-labeled anti-HER2 sdAb (^{99m}Tc-NM-02) and examined its use as a novel tracer for SPECT/CT assessment of HER2 expression in breast cancer patients.

Results

Radiopharmaceutical preparation

^{99m}Tc-NM-02 was readily prepared with high radiochemical purity (RCP). The mean RCP was 97.7 ± 1.2% (95.4–99.3%, n = 10), and further purification after radiolabeling was not necessary. The final injection solution was colorless with endotoxin levels below 0.9 EU/mL.

Patient Characteristics

Between September 2019 and August 2020, 10 female breast cancer patients at first diagnosis, at relapse, or under treatment, participated in this study. All tissue samples used for pathologic HER2 testing were obtained less than 15 days prior to imaging. Five patients had no HER2 expression, and 5 patients had moderate or high expression of HER2 on IHC (2 + or 3+). Three of 10 patients had only primary tumors, and the other 7 patients had both primary tumors and metastases. The patient characteristics are summarized in Table 1.

Table 1
Patient characteristics

Patient no.	Age (y)	IA (MBq)	Tumor type	ER/PR	HER2 IHC	HER2 FISH		Tumor size (cm)	Primary tumor position	Metastatic lesion	Clinical staging
						Positivity	Ratio				
BR001	53	509.9	IPC	-/-	3+	A	A	2.9×5.4×4.7	right	right axillary lymph node	T3N1M0
BR002	47	499.9	IDC	-/-	0	-	0.88	1.8×1.3×1.6	bilateral	left axillary lymph nodes	T1cN1M0
BR003	41	409.6	IDC	+/+	0	-	1.06	3.5×6.1×2.7	bilateral	bilateral axillary lymph nodes	T3cN2aM0
BR004	51	472.1	IDC	+/-	0	-	0.88	2.0×1.8×2.0	left	NA	T2N0M0
BR005	66	405.5	IDC	-/-	0	-	1.27	4.0×3.0×2.0	left	NA	T1N0M0
BR006	50	485.4	IDC	+/-	3+	A	A	7.0×3.0×3.5	right	right axillary lymph nodes and right supraclavicular nodes	T4bcN3cM0
BR007	62	465.8	ILC	+/+	0	-	1.08	1.0×0.5×0.5	left	NA	T1bN0M0
BR008	57	421.8	IDC	+/+	2+	-	1.53	2.5×1.5×1.3	left	left axillary lymph node	T2N1M0
BR009	54	465.8	IDC	+/+	2+	-	1.05	3.1×2.0×3.3	right	right axillary lymph node	T2N1M0
BR010	41	446.2	IDC	+/+	3+	+	1.17	8.1×2.0×5.5	right	right axillary lymph nodes	T3cN2aM0

IA = injected activity; ER = estrogen receptor; PR = progesterone receptor; IPC = invasive papillary carcinoma; IDC = invasive ductal carcinoma; ILC = invasive lobular carcinoma; A = absent. Clinical staging was determined using the eighth edition of the American Joint Committee on Cancer staging for breast cancer.

Safety Assessment

No signs or symptoms of drug-related adverse effects were reported during the 1-week post-injection follow-up period. Clinical blood tests showed no significant changes that could be related to the study drug.

Biodistribution

Figure 1 shows the whole-body SPECT images of a representative patient at different time points. ^{99m}Tc-NM-02 was mainly observed in the liver and kidneys, with mild uptake in the spleen, intestines, and glandular tissues such as the thyroid, submandibular, and parotid glands.

This biodistribution pattern was already present at 10 min post-injection and decreased over time. Notably, fast clearance was seen in the lung and blood, with only a very low level of radioactivity remaining at 1 h post-injection, allowing improved tumor-to-background signal within 2 h after injection. Although there was radiotracer uptake in the liver and intestines, there were no signs of hepatobiliary excretion, such as an accumulation in the gallbladder or duodenum. In contrast, high uptake in the kidneys and continuous excretion of activity into the bladder could be clearly seen during the studied time period.

Radiation Dosimetry

Table 2 summarizes the individual organ doses and individual effective doses for three patients involved in the dosimetry study. The kidneys showed the highest organ dose (0.031 ± 0.0021 mSv/MBq), followed by the thyroid (0.019 ± 0.0050 mSv/MBq) and liver (0.014 ± 0.0019 mSv/MBq). Time activity curves for the six organs with the highest radiotracer uptake are shown in Fig. 2. The mean effective dose was 6.56×10^{-3} mSv/MBq.

Table 2
Organ radiation doses

Organ/Tissue	Mean (mSv/MBq)	SD (mSv/MBq)
Adrenals	5.00E-03	4.42E-04
Brain	1.00E-03	1.16E-04
Breasts	1.00E-03	1.33E-04
Gallbladder	6.00E-03	7.64E-04
Heart	3.00E-03	3.19E-04
Kidneys	3.10E-02	2.02E-03
Liver	1.40E-02	1.91E-03
LLI	7.00E-03	3.65E-03
Lungs	5.00E-03	3.79E-03
Muscle	2.00E-03	1.83E-04
Osteogenic Cells	5.00E-03	5.39E-04
Ovaries	3.00E-03	8.64E-04
Pancreas	5.00E-03	4.15E-04
Red Marrow	2.00E-03	1.46E-04
Skin	1.00E-03	1.14E-04
Small	4.00E-03	9.27E-04
Spleen	1.10E-02	1.09E-03
Stomach	4.00E-03	6.22E-04
Thymus	2.00E-03	1.37E-04
Thyroid	1.90E-02	5.02E-03
ULI	9.00E-03	4.09E-03
Urinary	3.00E-03	8.78E-04
Uterus	3.00E-03	4.42E-04
Effective Dose	6.56E-03	6.91E-04

Tumor Imaging

The SPECT/CT images of all patients were carefully evaluated by visual interpretation (Table 3). Other than one HER2-negaitive patient (Patient BR007) who showed no distinct uptake in the tumor, nine patients had varying degrees of tracer uptake in their primary tumors, and the tumors were classified as positive based on imaging results. The obvious tumor uptake in the primary tumors of the five HER2-positive patients was consistent with their IHC results (HER2 2 + or 3+). Figure 3 shows the representative images of Patient BR007 (HER2 0) who had no distinct tumor uptake, and Patient BR001 (HER2 3+) who had high tracer accumulation in the primary lesions. Moreover, the tracer accumulation observed in Patient BR001 matched well with the uptake patterns of a recent ^{18}F-FDG scan (Fig. S1). The remaining four HER2-negative patients (HER2 0) had visually evident uptake in the primary tumors, but varying levels of intensity were observed in different tumor areas, suggesting intratumoral heterogeneity in HER2 expression. Fig. S2 shows a representative case of tumor heterogeneity (Patient BR005). Tracer accumulation was also observed in the metastases with varying degrees of uptake. Figure 4 shows the images of Patient 6 (HER2 3+) and Patient 10 (HER2 3+), both of whom had clear tracer accumulation in their primary lesions but different uptake levels in their metastases, which may reflect intertumoral heterogeneity in HER2 expression [27, 28].

Table 3
Imaging characteristics

Patient no.	HER2 IHC	Visual interpretation				SUV_{max} of tumor lesions			
		primary		metastatic		primary		metastatic	
		1 h	2 h	1 h	2 h	1 h	2 h	1 h	2 h
BR001	3+	+	+	-	-	2.41	4.70	0.64	0.35
BR002	0	-/+	-/+	-	-	0.66/3.16	0.92/2.71	0.71	0.44
BR003	0	+/+	+/+	+/+	+/+	4.06/3.97	5.80/3.33	4.42/2.24	3.81/2.83
BR004	0	+	+	NA		3.29	4.25	NA	
BR005	0	+	+	NA		1.92	1.81	NA	
BR006	3+	+	+	+/+	+/+	8.92	11.18	5.00/6.20	5.83/8.55
BR007	0	-	-	NA		0.76	1.34	NA	
BR008	2+	-	+	+	+	1.36	1.76	1.80	2.87
BR009	2+	+	+	+	+	6.95	8.17	3.59	4.72
BR010	3+	+	+	+	+	6.21	7.89	8.18	10.70
NA = Not applicable									

In addition to visual interpretation, the tracer uptake was quantitatively analyzed, and the maximal standard uptake values (SUV_{max}) are recorded in Table 3. The SUV_{max} ranged from 0.64 to 8.92 at 1 h post-injection and 0.35 to 11.18 at 2 h post-injection. The SUV_{max} in the primary tumors was greater at 2 h than at 1 h (average, 4.49 vs. 3.64, $P < 0.05$), and a similar trend was also observed in the metastases (average, 4.46 vs. 3.64, $P < 0.05$). When an SUV_{max} of 1.5 was used as a threshold for positivity, the visual interpretations and quantitative analyses were concordant in all patients at the studied timepoints. Notably, the imaging result of Patient BR008 (HER2 2+) was considered to be negative by visual interpretation at 1 h, but it was positive at 2 h, suggesting the necessity of delayed imaging for the patients with equivocal uptakes. This was consistent with the increased SUV_{max} over time (1.36 vs. 1.76).

Discussion

HER2-positive breast cancer patients have poor prognosis due to the aggressive nature of HER2-positive disease [6]. Many studies have reported that HER2-targeted treatments, including anti-HER2 antibodies (such as trastuzumab and pertuzumab) and small-molecule tyrosine kinase inhibitors (such as lapatinib and neratinib), have excellent overall survival benefits in this patient cohort [1]. Therefore, determining the HER2 expression level in tumors is vital when selecting targeted therapy. Currently, this means analysis of HER2 expression by IHC and/or *HER2/neu* gene amplification by FISH. However, despite standardization of testing methods and interpretation recommendations, assessment of HER2 status can still be inaccurate. Several factors contribute to this imprecise HER2 interpretation, such as HER2 heterogeneity, gain in chromosome enumeration probe 17 copy number, and HER2 status alteration after neoadjuvant

chemotherapy or during metastatic progression [13]. As more therapeutics are approved for HER2-postive tumors, there is a growing need to accurately determine the HER2 status of both primary and metastatic tumors.

In this study, we utilized an accurate, whole-body and non-invasive method for HER2 status determination to help clinicians to identify breast cancer patients who will benefit from HER2-targeted therapy. This first-in-human study of ^{99m}Tc-NM-02 as a radiotracer for SPECT/CT assessment of HER2 expression was conducted in 10 female breast cancer patients. The safety of this tracer was excellent, with no reported adverse reactions and acceptable radiation dosimetry. The SPECT/CT data demonstrated favorable biodistribution and satisfactory imaging characteristics of ^{99m}Tc-NM-02. As with other radiolabeled sdAbs [23–25], the urinary system received the highest radiation dose, but it was tolerable. The radiation dosimetry of ^{99m}Tc-NM-02 was similar to that of the ^{99m}Tc-labeled anti-PD-L1 sdAb reported in our previous study [26]. Although the individual organ doses are acceptable for a diagnostic procedure and in line with other ^{99m}Tc-labeled radiotracers in clinical use [29], they could potentially be further minimized by faster excretion using methods such as co-injection of diuretic agents.

Some studies have attempted to decrease nonspecific radiotracer accumulation in the liver and spleen by increasing the dose of non-radiolabeled sdAb, but the effect was very limited [24]. In our previous study, we encountered similar results [26]. In that study, we observed no significant differences in image quality, biodistribution, and tumor-to-background ratios in patients receiving 100 and 400 μg of sdAb. Therefore, we injected 100 μg of NM-02 sdAb in this study. As anticipated, the ^{99m}Tc-NM-02 tracer mainly accumulated in the liver and kidneys, and increased activity in the bladder indicated that ^{99m}Tc-NM-02 was eliminated through the urinary system, in line with the excretion patterns described in the literature [24].

Although trace uptake in the liver, spleen, and intestines was visible early after injection, we observed rapid clearance from these organs at 1 h after injection, with no signs of hepatobiliary excretion, such as an enhanced accumulation in the gallbladder or duodenum. This might be explained by the rapid clearance of ^{99m}Tc-NM-02 from the blood pool. The rapid blood clearance not only allowed us to perform SPECT imaging at early time points (within 2 h after injection) but also might reduce the risk of false-positive signals due to high activity in the blood pool. In addition, there was rapid tracer reduction in normal lung tissue, which further improved the contrast of primary breast cancer and metastases in images. Because of this continuous and rapid decreasing activity in the blood pool and lung background over time, images acquired at 2 h after injection had higher signal-to-noise ratios than those acquired at 1 h.

Unlike the biodistribution data in our previous work [26], mild uptake of ^{99m}Tc-NM-02 was observed in the thyroid, submandibular, and parotid glands. This pattern has also been reported in other studies of similar tracers, such as the ^{68}Ga-labeled anti-HER2-nanobody and the ^{111}In-labeled anti-HER2-Affibody [24, 30, 31]. The tracer uptake may reflect the low-level HER2 expression in these glandular tissues, or it may be associated with chelator-mediated trapping mechanisms. However, studies performed with ^{18}F-anti-HER2-nanobody and ^{111}In-labeled anti-HER2 monoclonal antibody showed insignificant uptake in these glands [32–34]. Notably, glandular uptake has also been reported in prostate-specific membrane antigen and fibroblast-activating protein inhibitor tracers [35, 36]. These results reveal the complex mechanisms of glandular uptake, and its cause remains unknown.

The SPECT/CT images of primary lesions and metastases were carefully evaluated in these breast cancer patients and compared with their HER2 IHC results. As expected, five patients with positive HER2 IHC results had obvious tracer uptake in their primary lesions. Remarkably, four of five HER2-negative patients in this study also showed obvious local tracer uptake in their primary tumors, likely due to the intratumoral heterogeneity of HER2 expression. This discordance in uptake might be due to the tumor specimens being obtained by core needle biopsy from a small area of the tumor, which fails to capture the heterogeneity within the tumor. Additionally, intertumoral heterogeneity was observed in some patients with metastases. Distinct uptake was seen in the metastases of seven patients, although the primary tumor of one patient (Patient BR003) was classified as HER2-negative based on pathology results. Conversely, one patient (Patient BR001) with inconspicuous tracer uptake in metastases had high HER2 expression (HER2 3+) in the primary lesion. The inconsistency of tracer uptake in metastases could be attributable to a discordance in HER2 expression between the primary tumor and the metastases, which has been previously reported [37, 38]. This intra- and intertumoral heterogeneity in HER2 expression highlights the need for the development of non-invasive imaging methods to provide more holistic information on HER2 status when making HER2-targeted therapy decisions.

Tumor uptake in the primary lesions and metastases of these breast cancer patients showed a wide range of SUV_{max} (0.35–11.18). Although it was not the primary purpose of this early phase I study, based on these SUV_{max}, we attempted to identify a cutoff for determining HER2 positivity in SPECT/CT imaging. An SUV_{max} of 1.5 appeared to be a reasonable point. Using this cutoff, the results of visual interpretation from nuclear medicine doctors and the tumor SUV_{max} at both 1 h and 2 h post-injection were consistent. Interestingly, Patient BR008 was originally identified to have a HER2-negative tumor based on imaging by visual interpretation at 1 h post-injection, but

the tumor was redefined at 2 h post-injection (SUV_{max} of 1.36 and 1.76, respectively). This suggested not only the utility of the identified cutoff value but also the importance of delayed imaging for the patients with equivocal uptakes.

Several researchers have discussed the advantages of sdAbs as novel candidates in the development of molecular imaging tracers when compared with full therapeutic antibodies [16]. Based on these distinctive properties, many researchers have labeled various anti-HER2 sdAbs and antibodies with different radionuclides for PET and SPECT imaging, including ^{89}Zr, ^{64}Cu, ^{68}Ga and ^{111}In [23, 24, 39–41]. However, the availability and production costs of these radionuclides may hinder their rapid clinical transformation and popularization. In this situation, ^{99m}Tc-labeled sdAbs can be translated into clinical application with more ease, thanking to the ideal properties and popularity of ^{99m}Tc radionuclide [42].

Although the relatively small sample size of this study is a potential limitation, this study provided sufficient pilot feasibility data on the optimal imaging time point, radiation dosimetry analysis, biodistribution pattern, and, most importantly, safety of this novel tracer. Moreover, recent advances in targeted radionuclide therapy for HER2-overexpressing tumors using radiolabeled sdAbs displayed impressive results [43, 44]. This sdAb is planned to be studied in larger clinical trials for non-invasive detection of HER2 expression and targeted radionuclide therapy in breast cancer [45, 46].

Conclusions

^{99m}Tc-NM-02 was safely administered and imaged in 10 breast cancer patients with acceptable radiation dosimetry. A clear tumor signal was obtained in primary lesions and metastases within 2 h after injection. An SUV_{max} of 1.5 could be a reasonable cutoff for determining HER2 positivity in SPECT/CT imaging. ^{99m}Tc-NM-02 SPECT imaging may provide an accurate and non-invasive method to detect HER2 status for breast cancer patients. Future studies with larger cohorts are warranted to make more meaningful comparisons between imaging and pathologic HER2 expression results.

Methods

Radiopharmaceutical preparation

NM-02 selection and preparation was performed as previously described [26]. ^{99m}Tc-NM-02 was synthesized following the methodology published in the literature [26, 47]. Briefly, the $[^{99m}Tc(OH_2)_3(CO)_3]^+$ complex was first manufactured and added to a sealed vial containing 200 μg of NM-02. After incubation at 50°C for 1 h, the ^{99m}Tc-NM-02 was prepared, and a small amount of sample was withdrawn for quality control analysis. The RCP was analyzed using instant thin-layer chromatography, and endotoxin analysis was performed using Limulus Ameboctye Lysate testing. Additional File 1 includes additional details on the preparation of the radiopharmaceutical.

Patients

This was an open-label, non-randomized early phase I (first-in-human) study in 10 breast cancer patients. This study was registered at ClinicalTrials.gov (NCT04040686) and approved by the Shanghai General Hospital Ethics Committee. Informed consent was obtained from all patients enrolled in this study. Details of patient screening are included in Additional File 1.

Spect/CT Imaging

Ten patients were injected with 458 ± 37 MBq ^{99m}Tc-NM-02, corresponding to 100 μg of NM-02 nanobody, as an intravenous bolus. After injection, all patients were asked to drink more than 500 mL of water and empty their bladders before imaging to facilitate tracer clearance in normal tissue. All images were obtained using a GE Discovery NM670 SPECT/CT system (Denver, CO, USA). Routine whole-body SPECT images were acquired at 1 and 2 h post-injection for all patients. Images were also acquired at 10 min, 3 h, and 24 h after injection in three patients to calculate radiation dosimetry. At 1 h and 2 h post-injection, local SPECT/CT images of primary lesions and regional metastases were acquired. Visual interpretation of the images was performed by at least two experienced nuclear medicine doctors. Positive imaging was defined as focal ^{99m}Tc-NM-02 uptake greater than background corresponding to a lesion on conventional imaging. Negative imaging was defined as no distinct pathological tracer uptake. Tumor uptake was quantitatively analyzed using Q.Metrix software (Denver, CO, USA), and the SUV_{max} of tumor lesions were calculated at 1 and 2 h post-injection. The parameters used for SPECT/CT image acquisition and analysis are specified in Additional File 1.

Radiation Dosimetry Calculations

Radiation dosimetry calculations were performed as previously describe [26]. Three patients underwent additional whole-body planar imaging at 10 min, 3 h, and 24 h post-injection. A calibration source of 37 MBq was placed above the head of each patient at the time of injection to provide quantitative calibration of counts to activity. Radiation dosimetry calculations were performed by an experienced operator using OLINDA/EXM dose calculation software (version 1.1) and well-known models [48, 49].

Statistics

Data are reported as mean ± standard deviation and were analyzed using SPSS software (Version 24.0). One-way analysis of variance was performed to evaluate the significance of the data. A P value of less than 0.05 was considered statistically significant.

Abbreviations

HER2: human epidermal growth factor receptor 2; IHC: immunohistochemistry; FISH: fluorescence in situ hybridization; sdAb: single-domain antibody; PD-L1: programmed death ligand-1; RCP: radiochemical purity; SUV_{max}: maximal standard uptake value; PBS: phosphate-buffered saline; ITLC: instant thin-layer chromatography; R_f: retention factor

Declarations

Acknowledgements

We are grateful to Shanghai Nanomab Technology Limited for the help in NM-02 preparation.

Author Contributions

LZ Zhao: Data curation, Formal analysis, Investigation, Visualization, Methodology, Writing-original draft, Writing review and editing. CC Liu: Data curation, Formal analysis, Investigation, Methodology, Visualization, Writing review and editing. Y Xing: Investigation, Visualization. J He: Methodology. J O' Doherty: Methodology, Validation. WH Huang: Conceptualization, Data curation, Investigation, Supervision, Project administration. JG Zhao: Conceptualization, Investigation, Visualization, Validation, Project administration, Supervision, Writing review and editing. All authors read and approved the final manuscript.

Funding

This research is supported by Clinical Research Plan of SHDC (SHDC2020CR2057B and 16CR3052A).

Availability of data and materials

All data generated or analyzed during this study are included in this published article.

Ethics approval and consent to participate

This study was registered in ClinicalTrials.gov (NCT04040686) and was approved by the Shanghai General Hospital Ethics Committee. Informed consent was obtained from all patients enrolled into this study.

Consent for publication

All authors agree to be published.

Competing interests

The authors declare that they have no competing interests.

References

1. Waks AG, Winer EP. Breast Cancer Treatment: A Review. JAMA. 2019;321(3):288-300.
2. Januškevičienė I, Petrikaitė V. Heterogeneity of breast cancer: The importance of interaction between different tumor cell populations. Life Sci. 2019;239:117009.
3. Sun Y, Zhao Z, Yang Z, Xu F, Lu H, Zhu Z, et al. Risk Factors and Preventions of Breast Cancer. Int J Biol Sci. 2017;13(11):1387-97.

4. Prat A, Pineda E, Adamo B, Galván P, Fernández A, Gaba L, et al. Clinical implications of the intrinsic molecular subtypes of breast cancer. Breast. 2015;24:S26-S35.
5. Harbeck N, Gnant M. Breast cancer. Lancet. 2017;389(10074):1134-50.
6. Harbeck N, Penault-Llorca F, Cortes J, Gnant M, Houssami N, Poortmans P, et al. Breast cancer. Nat Rev Dis Primers. 2019;5(1):66.
7. Stover DG, Wagle N. Precision Medicine in Breast Cancer: Genes, Genomes, and the Future of Genomically Driven Treatments. Current Oncology Reports. 2015;17(4):15.
8. Loibl S, Gianni L. HER2-positive breast cancer. Lancet. 2017;389(10087):2415-29.
9. Rachel W, Nadia H. Neoadjuvant Therapy for HER2-positive Breast Cancer. Rev Recent Clin Trials. 2017;12(2):81-92.
10. Escrivá-de-Romaní S, Arumí M, Bellet M, Saura C. HER2-positive breast cancer: Current and new therapeutic strategies. Breast. 2018;39:80-8.
11. Oh D, Bang Y. HER2-targeted therapies-a role beyond breast cancer. Nat Rev Clin Oncol. 2020;17(1):33-48.
12. Murthy RK, Loi S, Okines A, Paplomata E, Hamilton E, Hurvitz SA, et al. Tucatinib, Trastuzumab, and Capecitabine for HER2-Positive Metastatic Breast Cancer. N Engl J Med. 2020;382(7):597-609.
13. Ahn S, Woo JW, Lee K, Park SY. HER2 status in breast cancer: changes in guidelines and complicating factors for interpretation. J Pathol Transl Med. 2020;54(1):34-44.
14. Phillips KA, Marshall DA, Haas JS, Elkin EB, Liang S, Hassett MJ, et al. Clinical practice patterns and cost effectiveness of human epidermal growth receptor 2 testing strategies in breast cancer patients. Cancer. 2009;115(22):5166-74.
15. Pfitzner BM, Lederer B, Lindner J, Solbach C, Engels K, Rezai M, et al. Clinical relevance and concordance of HER2 status in local and central testing—an analysis of 1581 HER2-positive breast carcinomas over 12 years. Mod Pathol. 2018;31(4):607-15.
16. Salvador JP, Vilaplana L, Marco MP. Nanobody: outstanding features for diagnostic and therapeutic applications. Anal Bioanal Chem. 2019;411(9):1703-13.
17. Chakravarty R, Goel S, Cai W. Nanobody: The "Magic Bullet" for Molecular Imaging? Theranostics. 2014;4(4):386-98.
18. Vaneycken I, Devoogdt N, Van Gassen N, Vincke C, Xavier C, Wernery U, et al. Preclinical screening of anti-HER2 nanobodies for molecular imaging of breast cancer. FASEB J. 2011;25(7):2433-46.
19. Zhou Z, Vaidyanathan G, McDougald D, Kang CM, Balyasnikova I, Devoogdt N, et al. Fluorine-18 Labeling of the HER2-Targeting Single-Domain Antibody 2Rs15d Using a Residualizing Label and Preclinical Evaluation. Mol Imaging Biol. 2017;19(6):867-77.
20. Dekempeneer Y, Bäck T, Aneheim E, Jensen H, Puttemans J, Xavier C, et al. Labeling of Anti-HER2 Nanobodies with Astatine-211: Optimization and the Effect of Different Coupling Reagents on Their in Vivo Behavior. Mol Pharm. 2019;16(8):3524-33.
21. Pruszynski M, D'Huyvetter M, Bruchertseifer F, Morgenstern A, Lahoutte T. Evaluation of an Anti-HER2 Nanobody Labeled with ^{225}Ac for Targeted α-Particle Therapy of Cancer. Mol Pharm. 2018;15(4):1457-66.
22. Bridoux J, Broos K, Lecocq Q, Debie P, Martin C, Ballet S, et al. Anti-human PD-L1 Nanobody for Immuno-PET Imaging: Validation of a Conjugation Strategy for Clinical Translation. Biomolecules. 2020;10(10):1388.
23. Xavier C, Vaneycken I, D'huyvetter M, Heemskerk J, Keyaerts M, Vincke C, et al. Synthesis, Preclinical Validation, Dosimetry, and Toxicity of ^{68}Ga-NOTA-Anti-HER2 Nanobodies for iPET Imaging of HER2 Receptor Expression in Cancer. J Nucl Med. 2013;54(5):776-84.
24. Keyaerts M, Xavier C, Heemskerk J, Devoogdt N, Everaert H, Ackaert C, et al. Phase I Study of ^{68}Ga-HER2-Nanobody for PET/CT Assessment of HER2 Expression in Breast Carcinoma. J Nucl Med. 2016;57(1):27-33.
25. Xavier C, Blykers A, Laoui D, Bolli E, Vaneyken I, Bridoux J, et al. Clinical Translation of [^{68}Ga]Ga-NOTA-anti-MMR-sdAb for PET/CT Imaging of Protumorigenic Macrophages. Mol Imaging Biol. 2019;21(5):898-906.
26. Xing Y, Chand G, Liu C, Cook GJR, O'Doherty J, Zhao L, et al. Early Phase I Study of a ^{99m}Tc-Labeled Anti–Programmed Death Ligand-1 (PD-L1) Single-Domain Antibody in SPECT/CT Assessment of PD-L1 Expression in Non–Small Cell Lung Cancer. J Nucl Med. 2019;60(9):1213-20.
27. Risom T, Wang X, Liang J, Zhang X, Pelz C, Campbell LG, et al. Deregulating MYC in a model of HER2+ breast cancer mimics human intertumoral heterogeneity. J Clin Invest. 2020;130(1):231-46.
28. Zhang H, Wang Y, Wang Y, Wu D, Lin E, Xia Q. Intratumoral and intertumoral heterogeneity of HER2 immunohistochemical expression in gastric cancer. Pathol Res Pract. 2020;216(11):153229.
29. Mattsson S. Patient dosimetry in nuclear medicine. Radiat Prot Dosimetry. 2015;165(1-4):416-23.
30. Baum RP, Prasad V, Müller D, Schuchardt C, Orlova A, Wennborg A, et al. Molecular Imaging of HER2-Expressing Malignant Tumors in Breast Cancer Patients Using Synthetic ^{111}In- or ^{68}Ga-Labeled Affibody Molecules. J Nucl Med. 2010;51(6):892-7.

31. Sörensen J, Sandberg D, Sandström M, Wennborg A, Feldwisch J, Tolmachev V, et al. First-in-Human Molecular Imaging of HER2 Expression in Breast Cancer Metastases Using the ^{111}In-ABY-025 Affibody Molecule. J Nucl Med. 2014;55(5):730-5.
32. Vaidyanathan G, McDougald D, Choi J, Koumarianou E, Weitzel D, Osada T, et al. Preclinical Evaluation of ^{18}F-Labeled Anti-HER2 Nanobody Conjugates for Imaging HER2 Receptor Expression by Immuno-PET. J Nucl Med. 2016;57(6):967-73.
33. Xavier C, Blykers A, Vaneycken I, D'Huyvetter M, Heemskerk J, Lahoutte T, et al. ^{18}F-nanobody for PET imaging of HER2 overexpressing tumors. Nucl Med Biol. 2016;43(4):247-52.
34. Kurdziel KA, Mena E, McKinney Y, Wong K, Adler S, Sissung T, et al. First-in-human phase 0 study of ^{111}In-CHX-A"-DTPA trastuzumab for HER2 tumor imaging. J Transl Sci. 2019;5(2):10.15761/JTS.1000269.
35. Kesler M, Levine C, Hershkovitz D, Mishani E, Menachem Y, Lerman H, et al. ^{68}Ga-Labeled Prostate-Specific Membrane Antigen Is a Novel PET/CT Tracer for Imaging of Hepatocellular Carcinoma: A Prospective Pilot Study. J Nucl Med. 2019;60(2):185-91.
36. Lindner T, Altmann A, Krämer S, Kleist C, Loktev A, Kratochwil C, et al. Design and Development of ^{99m}Tc-Labeled FAPI Tracers for SPECT Imaging and 188Re Therapy. J Nucl Med. 2020;61(10):1507-13.
37. Aurilio G, Disalvatore D, Pruneri G, Bagnardi V, Viale G, Curigliano G, et al. A meta-analysis of oestrogen receptor, progesterone receptor and human epidermal growth factor receptor 2 discordance between primary breast cancer and metastases. Eur J Cancer. 2014;50(2):277-89.
38. Yeung C, Hilton J, Clemons M, Mazzarello S, Hutton B, Haggar F, et al. Estrogen, progesterone, and HER2/neu receptor discordance between primary and metastatic breast tumours-a review. Cancer Metastasis Rev. 2016;35(3):427-37.
39. Laforest R, Lapi SE, Oyama R, Bose R, Tabchy A, Marquez-Nostra BV, et al. [^{89}Zr]Trastuzumab: Evaluation of Radiation Dosimetry, Safety, and Optimal Imaging Parameters in Women with HER2-Positive Breast Cancer. Mol Imaging Biol. 2016;18(6):952-9.
40. Ulaner GA, Lyashchenko SK, Riedl C, Ruan S, Zanzonico PB, Lake D, et al. First-in-Human Human Epidermal Growth Factor Receptor 2–Targeted Imaging Using ^{89}Zr-Pertuzumab PET/CT: Dosimetry and Clinical Application in Patients with Breast Cancer. J Nucl Med. 2018;59(6):900.
41. Lam K, Chan C, Reilly RM. Development and preclinical studies of ^{64}Cu-NOTA-pertuzumab F(ab')2 for imaging changes in tumor HER2 expression associated with response to trastuzumab by PET/CT. MAbs. 2017;9(1):154-64.
42. Duatti A. Review on ^{99m}Tc radiopharmaceuticals with emphasis on new advancements. Nucl Med Biol. 2021;92:202-16.
43. D'Huyvetter M, De Vos J, Xavier C, Pruszynski M, Sterckx YGJ, Massa S, et al. ^{131}I-labeled Anti-HER2 Camelid sdAb as a Theranostic Tool in Cancer Treatment. Clin Cancer Res. 2017;23(21):6616-28.
44. D'Huyvetter M, Vincke C, Xavier C, Aerts A, Impens N, Baatout S, et al. Targeted radionuclide therapy with A ^{177}Lu-labeled anti-HER2 nanobody. Theranostics. 2014;4(7):708-20.
45. Bensch F, Brouwers AH, Lub-de Hooge MN, de Jong JR, van der Vegt B, Sleijfer S, et al. ^{89}Zr-trastuzumab PET supports clinical decision making in breast cancer patients, when HER2 status cannot be determined by standard work up. Eur J Nucl Med Mol Imaging. 2018;45(13):2300-6.
46. Gebhart G, Lamberts LE, Wimana Z, Garcia C, Emonts P, Ameye L, et al. Molecular imaging as a tool to investigate heterogeneity of advanced HER2-positive breast cancer and to predict patient outcome under trastuzumab emtansine (T-DM1): the ZEPHIR trial. Ann Oncol. 2016;27(4):619-24.
47. Zhao L, Zhu J, Wang T, Liu C, Song N, Wu S, et al. A novel Buthus martensii Karsch chlorotoxin derivative for glioma SPECT imaging. New J Chem. 2020;44(35):14947-52.
48. Hindorf C, Glatting G, Chiesa C, Lindén O, Flux G. EANM Dosimetry Committee guidelines for bone marrow and whole-body dosimetry. Eur J Nucl Med Mol Imaging. 2010;37(6):1238-50.
49. Stabin MG, Sparks RB, Crowe E. OLINDA/EXM: The Second-Generation Personal Computer Software for Internal Dose Assessment in Nuclear Medicine. J Nucl Med. 2005;46(6):1023-7.

Tables

Table 1 Patient characteristics

Patient no.	Age (y)	IA (MBq)	Tumor type	ER/PR	HER2 IHC	HER2 FISH		Tumor size (cm)	Primary tumor position	Metastatic lesion	Clinical staging
						Positivity	Ratio				
BR001	53	509.9	IPC	-/-	3+	A	A	2.9×5.4×4.7	right	right axillary lymph node	T3N1M0
BR002	47	499.9	IDC	-/-	0	-	0.88	1.8×1.3×1.6	bilateral	left axillary lymph nodes	T1cN1M0
BR003	41	409.6	IDC	+/+	0	-	1.06	3.5×6.1×2.7	bilateral	bilateral axillary lymph nodes	T3cN2aM0
BR004	51	472.1	IDC	+/-	0	-	0.88	2.0×1.8×2.0	left	NA	T2N0M0
BR005	66	405.5	IDC	-/-	0	-	1.27	4.0×3.0×2.0	left	NA	T1N0M0
BR006	50	485.4	IDC	+/-	3+	A	A	7.0×3.0×3.5	right	right axillary lymph nodes and right supraclavicular nodes	T4bcN3cM0
BR007	62	465.8	ILC	+/+	0	-	1.08	1.0×0.5×0.5	left	NA	T1bN0M0
BR008	57	421.8	IDC	+/+	2+	-	1.53	2.5×1.5×1.3	left	left axillary lymph node	T2N1M0
BR009	54	465.8	IDC	+/+	2+	-	1.05	3.1×2.0×3.3	right	right axillary lymph node	T2N1M0
BR010	41	446.2	IDC	+/+	3+	+	1.17	8.1×2.0×5.5	right	right axillary lymph nodes	T3cN2aM0

IA = injected activity; ER = estrogen receptor; PR = progesterone receptor; IPC = invasive papillary carcinoma; IDC = invasive ductal carcinoma; ILC = invasive lobular carcinoma; A = absent. Clinical staging was determined using the eighth edition of the American Joint Committee on Cancer staging for breast cancer.

Table 2 Organ radiation doses

Organ/Tissue	Mean (mSv/MBq)	SD (mSv/MBq)
Adrenals	5.00E-03	4.42E-04
Brain	1.00E-03	1.16E-04
Breasts	1.00E-03	1.33E-04
Gallbladder	6.00E-03	7.64E-04
Heart	3.00E-03	3.19E-04
Kidneys	3.10E-02	2.02E-03
Liver	1.40E-02	1.91E-03
LLI	7.00E-03	3.65E-03
Lungs	5.00E-03	3.79E-03
Muscle	2.00E-03	1.83E-04
Osteogenic Cells	5.00E-03	5.39E-04
Ovaries	3.00E-03	8.64E-04
Pancreas	5.00E-03	4.15E-04
Red Marrow	2.00E-03	1.46E-04
Skin	1.00E-03	1.14E-04
Small	4.00E-03	9.27E-04
Spleen	1.10E-02	1.09E-03
Stomach	4.00E-03	6.22E-04
Thymus	2.00E-03	1.37E-04
Thyroid	1.90E-02	5.02E-03
ULI	9.00E-03	4.09E-03
Urinary	3.00E-03	8.78E-04
Uterus	3.00E-03	4.42E-04
Effective Dose	6.56E-03	6.91E-04

Table 3 Imaging characteristics

Patient no.	HER2 IHC	Visual interpretation				SUV_{max} of tumor lesions			
		primary		metastatic		primary		metastatic	
		1 h	2 h	1 h	2 h	1 h	2 h	1 h	2 h
BR001	3+	+	+	-	-	2.41	4.70	0.64	0.35
BR002	0	-/+	-/+	-	-	0.66/3.16	0.92/2.71	0.71	0.44
BR003	0	+/+	+/+	+/+	+/+	4.06/3.97	5.80/3.33	4.42/2.24	3.81/2.83
BR004	0	+	+	NA		3.29	4.25	NA	
BR005	0	+	+	NA		1.92	1.81	NA	
BR006	3+	+	+	+/+	+/+	8.92	11.18	5.00/6.20	5.83/8.55
BR007	0	-	-	NA		0.76	1.34	NA	
BR008	2+	-	+	+	+	1.36	1.76	1.80	2.87
BR009	2+	+	+	+	+	6.95	8.17	3.59	4.72
BR010	3+	+	+	+	+	6.21	7.89	8.18	10.70

NA = Not applicable

Figures

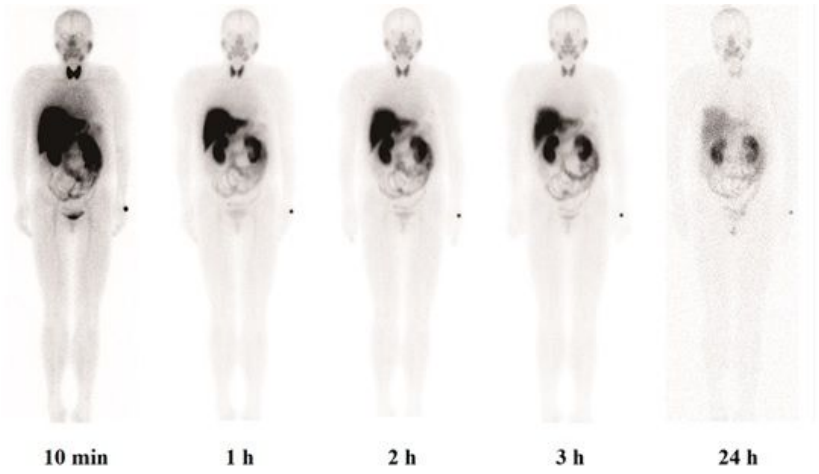

Figure 1

Anterior whole-body SPECT images of Patient BR001 at 10 min, 1 h, 2 h, 3 h, and 24 h after injection

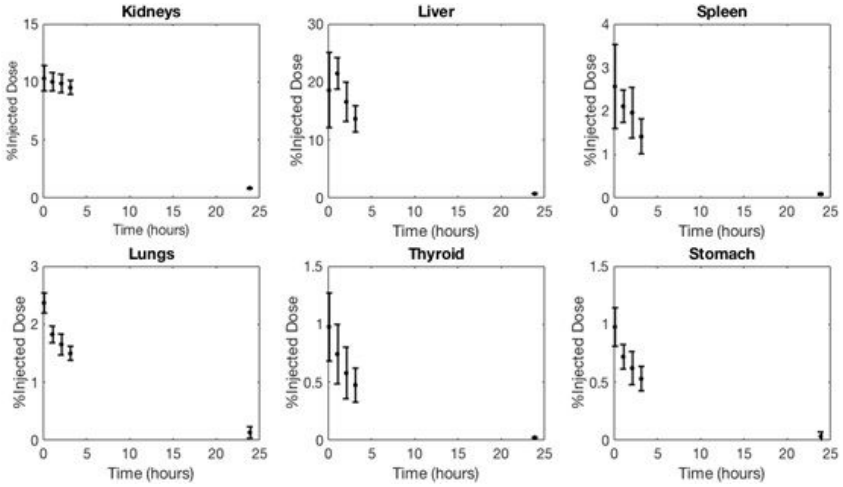

Figure 2

Time activity curve of organs with highest radiotracer uptake

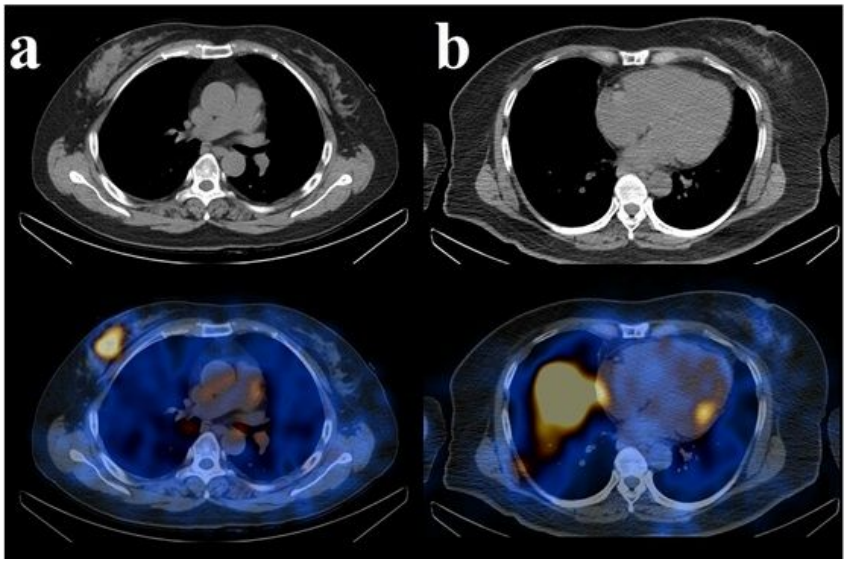

Figure 3

Representative SPECT/CT images of Patient BR001 (a) with high tracer accumulation and Patient BR007 (b) with no distinct tracer uptake in the primary lesions at 1 h after injection

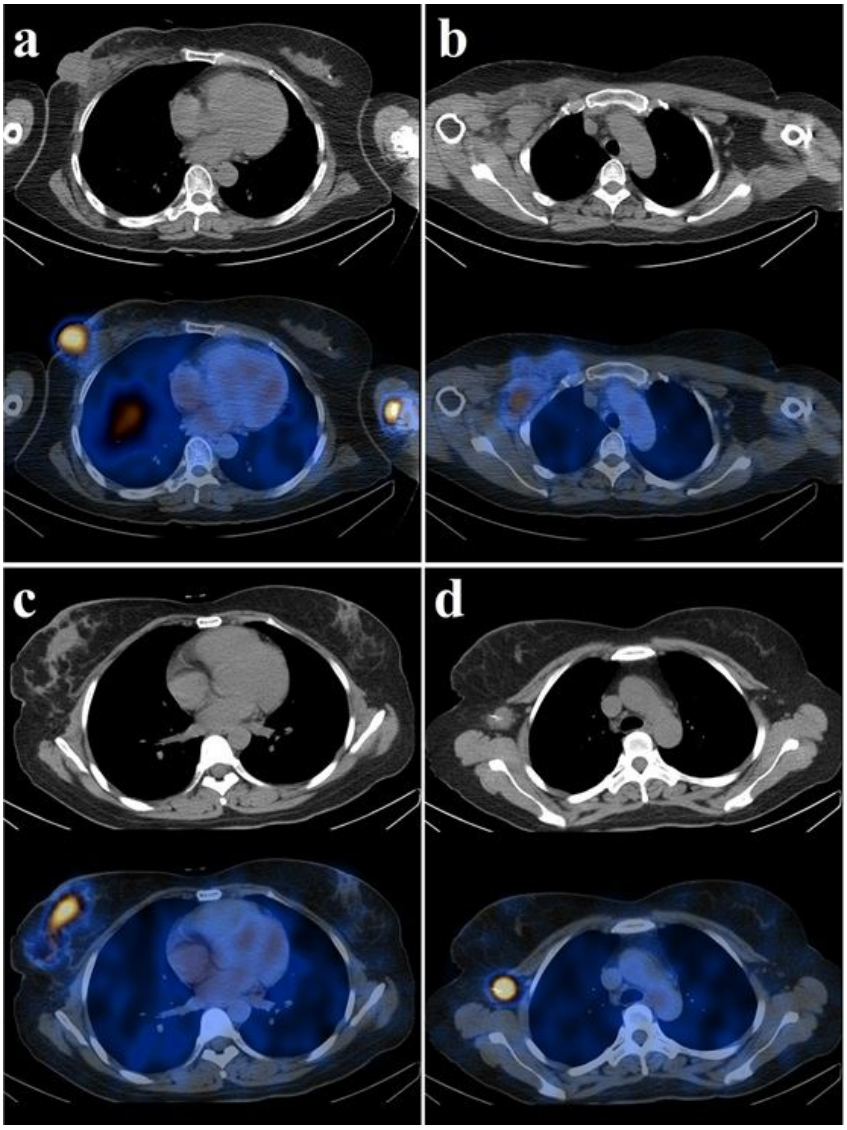

Figure 4

SPECT/CT images of Patient BR006 (a and b) and Patient BR010 (c and d) with evident radiotracer accumulation in the respective primary lesions (a and c) and varied intensities of radiotracer uptake in their metastases demonstrating heterogeneity of HER2 expression (b and d)

Supplementary Files

This is a list of supplementary files associated with this preprint. Click to download.

- SupplementaryMaterial.docx
- graphicalabstractimage.jpg